membranes

Review

Recent Progress of SAPO-34 Zeolite Membranes for CO_2 Separation: A Review

Muhammad Usman

Interdisciplinary Research Center for Hydrogen and Energy Storage (IRC-HES), King Fahd University of Petroleum & Minerals (KFUPM), Dhahran 31261, Saudi Arabia; muhammadu@kfupm.edu.sa

Abstract: In the zeolite family, the silicoaluminophosphate (SAPO)-34 zeolite has a unique chemical structure, distinctive pore size, adsorption characteristics, as well as chemical and thermal stability, and recently, has attracted much research attention. Increasing global carbon dioxide (CO_2) emissions pose a serious environmental threat to humans, animals, plants, and the entire environment. This mini-review summarizes the role of SAPO-34 zeolite membranes, including mixed matrix membranes (MMMs) and pure SAPO-34 membranes in CO_2 separation. Specifically, this paper summarizes significant developments in SAPO-34 membranes for CO_2 removal from air and natural gas. Consideration is given to a variety of successes in SAPO-34 membranes, and future ideas are described in detail to foresee how SAPO-34 could be employed to mitigate greenhouse gas emissions. We hope that this study will serve as a detailed guide to the use of SAPO-34 membranes in industrial CO_2 separation.

Keywords: zeolites; SAPO-34; membranes; CO_2 separation; molecular sieving; CO_2 mitigation

Citation: Usman, M. Recent Progress of SAPO-34 Zeolite Membranes for CO_2 Separation: A Review. *Membranes* **2022**, *12*, 507. https://doi.org/10.3390/membranes12050507

Academic Editors: Julio Garcia-Fayos, Cecilia Solís and María Balaguer

Received: 22 March 2022
Accepted: 28 April 2022
Published: 10 May 2022

1. Introduction

Anthropogenic activities are one of the primary causes of global warming. The primary cause of climate change is the combustion of fossil fuels, which results in enormous CO_2 concentration in the atmosphere. Recently, the CO_2 levels in the atmosphere were recorded as 414 parts per million, which is several folds higher than before the industrial revolution [1,2]. This increasing level of CO_2 causes the greenhouse effect, contributes to respiratory disease, acts as asphyxiant, causes ocean acidification, and acts as a major source of energy imbalance due to a rise in earth temperature. Several approaches have been developed to mitigate CO_2 in the atmosphere, including geological sequestration, catalytic conversion to useful products, adsorption, and membrane separation [3–6]. One approach is to separate and capture CO_2 from air and its originating sources.

Several gas separation strategies have been independently researched for CO_2 capture and separation, including cryogenic distillation and post-combustion processes such as absorption, adsorption, hydrated-based systems, and membrane separation techniques [7–9]. Cryogenic distillation necessitates huge distillation columns and is a high-energy process. Due to its compact footprint, simplicity, and great energy efficiency, membrane gas separation technology has been considered to be one of the most promising technologies to replace older technologies such as amine scrubbing. The membrane separation technique has considerable advantages over other separation technologies because it is a continuous separation process that consumes less energy, and the materials can be recycled. Recently, as compared with polymeric membranes, the incorporation of zeolites into polymers has been shown to improve CO_2 separation performance significantly.

In 1756, Swedish scientist Axel Fredrik Cronstedt invented the term "zeolite" [10]. Zeolites have a unique chemical composition, distinctive pore size distribution, and chemical, thermal, and ion exchange properties [11–21]. These materials have been employed for a range of applications, including capture, purification, and catalysis [22–30]. Among zeolites, Lok et al. [31] introduced the family of SAPO zeolite materials. The SAPO-34 unit cell has

chabazite (CHA)-type topology related to other aluminophosphates (such as SAPO-15, SAPO-11, SAPO-16, and SAPO-31), aluminosilicate (low-silica CHA and high-silica SSZ-13) and pure silicate (all-silica CHA). All these low and high-silica zeolite materials have been explored for gas separation applications [32–36].

The SAPO-34 zeolite has intra-crystalline pore volumes and pore sizes ranging from 0.18 to 0.48 cm^3/g and from 0.3 to 0.8 nm, respectively. The SAPO-34 structure is made up of eight-membered rings with a diameter of 9.4 (3.8 × 3.8), as shown in Figure 1. In addition to distinct pore size and volume, SAPO-34 material exhibits moderate to high hydrophobicity and has high thermal and hydrothermal stability. Due to these characteristic features, SAPO-34 has been extensively used in the methanol to olefin (MTO) process [37–48]. In recent years, SAPO-34 has been investigated for CO_2 remediation, including CO_2 capture [49–51], conversion [52–54], and separation [49]. Several studies have already covered a vast area of SAPO-34 materials research. Askari et al. [43] examined several synthetic procedures of SAPO-34. Ahmadi et al. summarized the deactivation of SAPO-34. Sun et al. looked at how to increase MTO performance in SAPO-34 by reducing the size of the zeolite using crystals and pore engineering. Furthermore, state-of-the-art SAPO-34 membranes and membranes reactor were addressed by Xu et al. [55]. Rimaz et al. proposed SAPO-34 as a best molecular sieve [56]. Kumar et al. studied CO_2 capture by different zeolites in general, whereas Singh et al. [39] explored porous materials for CO_2 capture applications. Kumar et al. [57] reviewed CO_2 capture by various zeolites in general. Recently, Usman et al. [54] reviewed SAPO-34 zeolite materials for CO_2 capture and conversion into useful chemicals. Despite the publication of multiple review studies, the role of SAPO-34 zeolite in CO_2 mitigation has yet to be summarized. There has been a lot of research done on SAPO-34 membranes for CO_2 separation, but no recent paper has been written about the role of SAPO-34 membranes in CO_2 separation, especially from air (N_2) and natural gas (CH_4). Therefore, this review was conceived as a result of the rapidly developing research on SAPO-34, as shown in Figure 2, and its role in CO_2 mitigation.

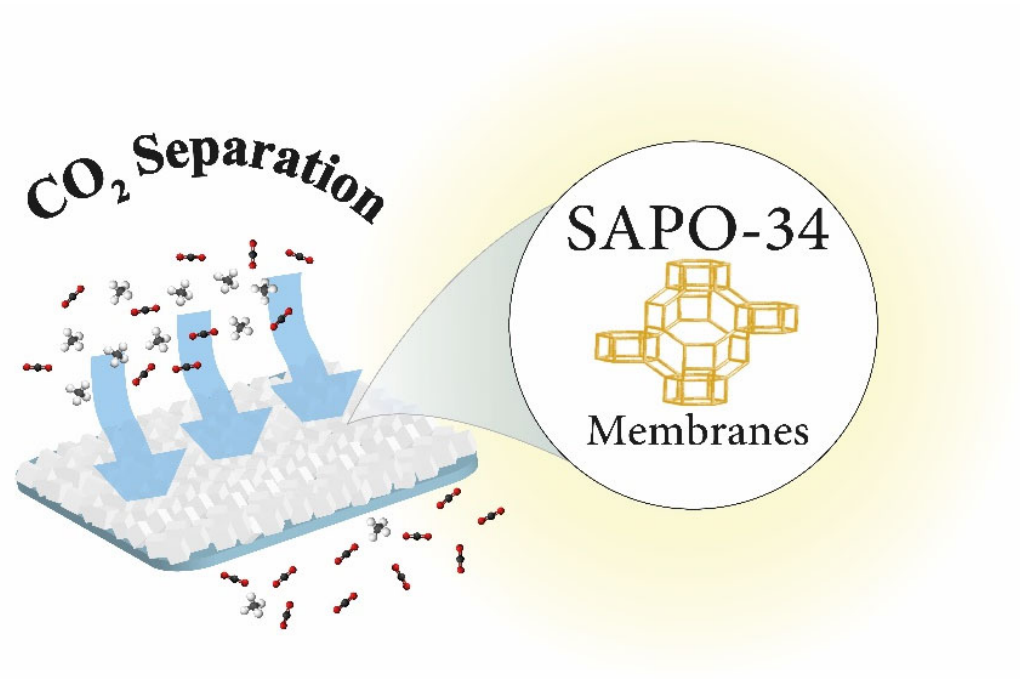

Figure 1. Schematic presentation of SAPO-34 membranes in CO_2 separation.

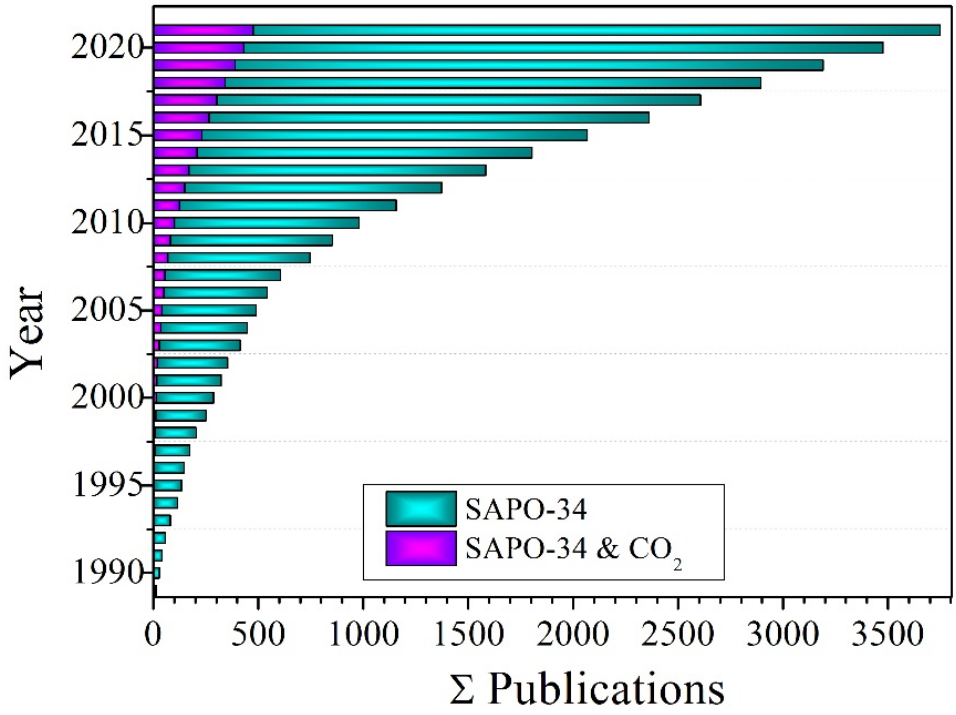

Figure 2. Histograms of SAPO-34 zeolite literature since 1990. Data were taken from SciFinder using keywords "SAPO-34" and "SAPO-34 and CO_2".

2. SAPO-34 Membranes for CO_2 Separation

A crystalline hydrate aluminosilicate is distinguished by its uniform pore size (0.3–1.3 nm), as well as superior thermal, chemical, and mechanical stability. Zeolite is an ideal material for different applications, such as adsorption, ion exchange, and catalysis. Recently, it has become attractive for membrane applications due to its unique structure and excellent physicochemical properties [58]. Among more than 190 zeolite frameworks, a few have been distinguished for their promising separation performances. SAPO-34 is one of these structures that exhibits a significant separation performance, specifically removing CO_2 from CH_4 and N_2 mixture. As shown in Figure 3, SAPO-34 membranes are mainly classified into two types: (1) Mixed matrix membranes (MMMs) where the SAPO-34 is incorporated in the polymer. These membranes are fabricated via various methods, including solution casting, phase inversion, solvent evaporation, and dip coating. (2) Pure SAPO-34 membranes where a substrate such as alumina, stainless steel, and silica are used as a support for the SAPO-34 membranes. Secondary seeded growth and in situ crystallization methods are the most frequent routes to fabricate these membrane types. In this review article, an extensive literature review about the separation and gas permeation of SAPO-34 membranes, in the last decade, is discussed including MMMs and pure membranes.

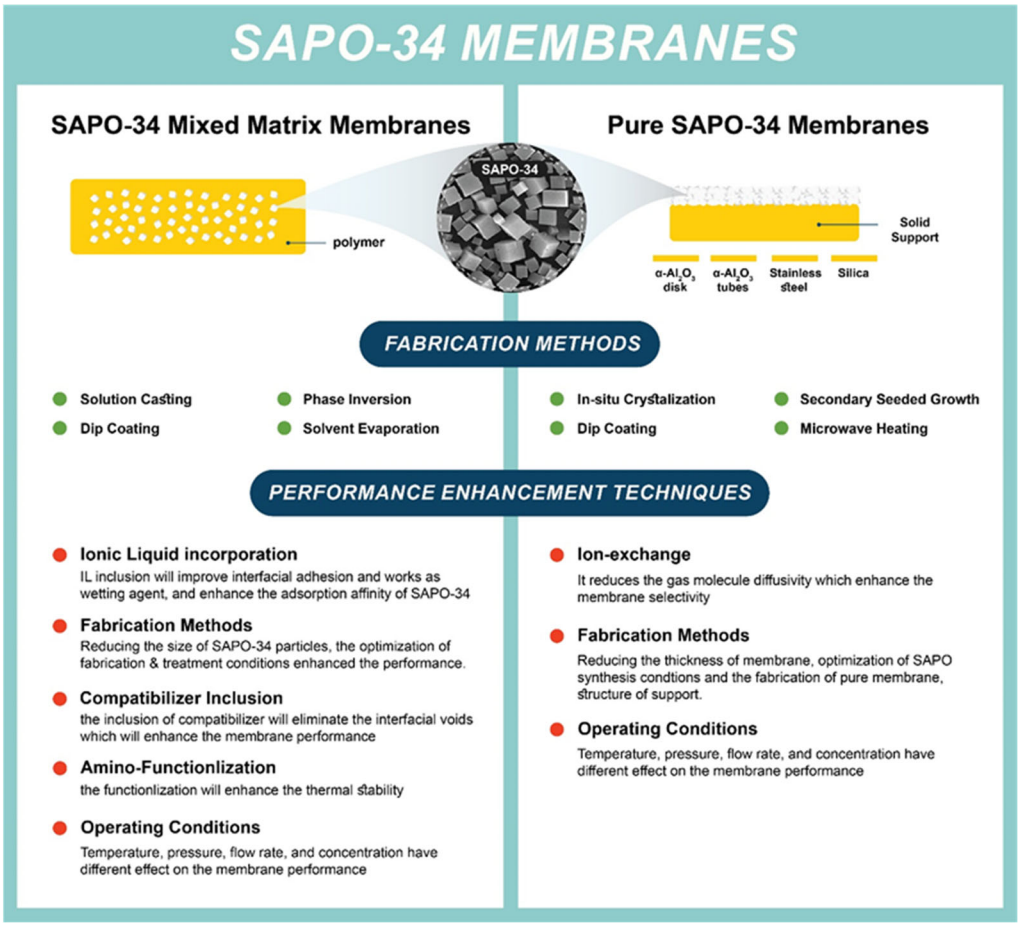

Figure 3. Schematic of fabrication method and performance advancement approaches for SAPO-34 membranes.

2.1. SAPO-34-Based Mixed Matrix Membranes

Several gas separation technologies have been investigated for CO_2 capture, including cryogenic distillation, post-combustion process, and membrane separation processes. Membrane separation technology shows significant merits as compared with other separation technologies because it is a continuous separation process, requires low energy consumption, and the materials can be regenerated. As compared with the polymeric membranes, MMMs that combine the advantages of both polymeric and inorganic materials have become the focus for a next-generation gas separation membrane. MMMs could provide a solution to the permeability and selectivity trade-off in polymeric membranes and bridge the gap with pure inorganic membranes. MMMs also offer the physicochemical stability of a ceramic material while ensuring the desired morphology with higher permeability, selectivity, hydrophilicity, fouling resistance, as well as greater thermal, mechanical, and chemical strength over a wider temperature and pH range. In MMMs where the flexibility, processability, and scalability of polymeric membranes meet the exceptional separation performance, the chemical and thermal stability of inorganic fillers have become a trending focus of academia and industry.

Since the first report of MMMs in 1970 [59], extensive research has been conducted to improve the separation performance and industrial implementation for a range of applications such as hydrogen recovery, treatment of natural gas, and air separation [60–62]. Different types of polymer matrices have been reported with various fillers, such as MOFs [63–67], COFs [68–72], carbon materials [73], zeolites [59], and other materials [74,75]. Zeolite materials with their sieving properties and cost-effectiveness on a large scale make them better

candidates for gas separation. The most suitable zeolite filler for CO_2 separation is SAPO-34 due to its unique structure and CO_2 adsorption affinity [76].

2.1.1. SAPO-34 MMMs

Peydayesh et al. [77] fabricated SAPO-34/Matrimid 5218 MMMs. They showed 55% and 97% enhancements in CO_2 permeability and CO_2/CH_4 selectivity, respectively, indicating the good adhesion of the filler in the polymer matrix. Wu et al. [78] reported an MMMs obtained by the inclusion of SAPO-34 nanoparticles within a polyethersulfone (PESU) polymer. The separation performance increased with increasing SAPO-34 loading. In addition, the nanoparticle size was investigated, where 100 nm particles resulted in defective membranes. In contrast, 200 nm SAPO-34 showed fewer defects with a continuous interface and higher permselectivity than smaller particles. Carter et al. [79] reported three types of filler: SAPO-34, silica, and ZIF-8. Among all the fabricated MMMs, ZIF-8 showed the best performance owing to the strong interaction between the filler and polymer matrix and surface diffusion transport. In addition, the study claimed that pore size was the most influential factor in gas permeability, as it increased permeability. As a result of the reduced interfacial voids and chain mobility, the SPAO-34 MMMs showed high ideal selectivity. Messaoud et al. [80] reported a dip-coating route for fabricating SAPO-34/polyetherimide MMMs. This study investigated the effects of two solvents, N-methyl-2-pyrrolidone (NMP) and dichloroethane (DCE), on membrane fabrication. DCE resulted in better performance properties related to the entrapping of small DCE molecules in SAPO-34 particles, which induced the sealing of SAPO-34 pores. The best molecular sieving performance was achieved with 5 wt% SAPO-34 MMMs with 4.41×10^{-10} mol m^{-2} s^{-1} Pa^{-1} and 60 CO_2/CH_4 selectivity. Particle agglomeration was observed with 10 wt% MMMs. Zhao et al. [81] reported SAPO-34/Pebax1657 MMMs fabricated by solvent evaporation. The inclusion of SAPO significantly enhanced the CO_2 permeability as compared with that of the neat membrane, whereas the selectivity remained constant. The effect of pressure was studied, and as a reason for plasticization, the permeation of MMMs increased with pressure. Junaidi et al. [82] conducted two studies on MMMs. First, asymmetric SAPO-34/PSf MMMs were prepared using the phase inversion method. The highest performance was achieved with 10 wt% MMMs with ideal selectivity 28.1 and 26.2 for CO_2/CH_4 and CO_2/N_2, respectively. When the filler loading was increased to >20 wt%, it led to poor interaction between filler and matrix which caused interfacial voids. They modified the SAPO-34 particles with the coupling agent APMS using two solvents, isopropanol and ethanol, before being added to the polymer matrix to overcome the previously reported challenge. The study showed that modified SAPO-34 MMMs exhibited better performance than unmodified and neat membranes owing to the reduction in interfacial voids [83]. An experimental and modeling study was reported by Santaniello et al. [76] where 200 nm SAPO-34 was incorporated, for the first time, in a polyhexafluoropropylene PHFP matrix. The MMMs with 24.6 v% and 36 v% showed an enhancement in the permeability and CH_4/CO_2 selectivity as compared with the neat membrane, which was ascribed to the increased polymer-free volume. The modeling part of gas transport confirmed the experimental results that 200 nm SAPO-34 particles provoked a polymer-free volume of 24.6 v%.

2.1.2. SAPO-34 Functionalized MMMs

The functionalization strategy offers the prospect of enhancing membrane performance. Cakal et al. [84] reported the influence of compatibilizer additives on the permeation performance of SAPO-34/HMA/PES membranes. The elimination of interfacial voids in the membrane is the main role of the HMA compatibilizer. The improvement in CO_2/CH_4 selectivity for SAPO-34 (20 wt%)/HMA (10%)/PES as compared with neat PES was attributed to the reduction in the diffusion pathway of CH_4. The effect of temperature was expected, as the permeability of all gases was enhanced as the temperature increased [85]. The effect of the functionalization of SAPO-34 with ethylenediamine (EDA) and hexylamine (HA) organic amino cations on the gas permeation, morphology, and pore size of

SAPO-34/PES MMMs was investigated. The MMMs fabricated with modified SAPO-34 with the EDA agent showed better performance than the HA agent owing to higher amino grafting, which enhanced the filler/polymer adhesion, resulting in a better CO_2/CH_4 ideal selectivity [86]. Amino functionalization and ionic liquid inclusion were studied by Nasir et al. [87]. The study revealed that the improvement of the particles/polymer interphase was due to the incorporation of [emim][Tf_2N] ionic liquids. Simultaneously, the amino functionalization of the SAPO-34 surface by EDA and HA enhanced the thermal stability of the MMMs. In addition, the membrane with the modified SAPO-34 and [emim][Tf_2N] IL exhibited the best CO_2/CH_4 selectivity as compared with that of the neat membrane. The hydrophobicity of MMMs is a key factor for industrial applications. Functionalization of SAPO-34 using 1H,1H,2H,2H-perflourodecyltriethoxysilane (HFDS) fluorocarbons was reported by Junaidi et al. [88]. In this study, functionalized SAPO-34 particles were embedded in a PSf polymer to overcome the competitive adsorption of moisture under wet conditions. Among the fabricated MMMs, the SAPO-34 10 wt% + 0.1 HFDS/PSF membrane showed the best performance (CO_2 permeance = 278 GPU) and (CO_2/CH_4 = 38.9) as compared with a bare polymer. The incorporation of modified SAPO-34 enhanced the membrane 17.64% hydrophobicity and showed better filler/polymer adhesion. In addition, SAPO-34 10 wt% + 0.1 HFDS/PSf membrane showed excellent stability for long-term stability tests under wet and dry conditions, whereas the unmodified membrane lost 90% of its performance under wet conditions.

Incorporating the third component in the MMM plays a vital role in improving SAPO-34 membrane performance. Nawar et al. reported the synergetic influence of ionic liquid (IL) inclusions on the separation of SAPO-34 MMMs [89]. In this study, 5 wt% SAPO-34 particles were incorporated into the polysulfone matrix, and the resulting membrane was immersed in 1-ethyl-3-methylimidazolium bis(tri-fluoromethylsulfonyl)imide IL. The membrane with the 0.2 M ionic liquid showed enhanced membrane performance as compared with the unmodified membrane, which was ascribed to interfacial defect reduction due to ionic liquid inclusion. Increasing the amount of ionic liquid caused a reduction in permeance and selectivity owing to pore and filler blockage. Ahmad et al. [90] used an [emim][TF2N] IL. Increasing the immersion time of SAPO-34 membranes led to an enhancement in the adsorption affinity of SAPO-34 for CO_2 and filler/polymer interfacial adhesion, and SAPO-34 + IL/PSF showed the best performance as compared with neat PSF, with ideal selectivity of 20.35 and 18.82 for CO_2/CH_4 and CO_2/N_2, respectively. Mohshim et al. [91] reported the use of Tf2N in SAPO-34/PES. This work also proved that ionic liquids improve interfacial adhesion and function as wetting agents. The performance of the modified MMMs was significantly enhanced as compared with bare PES. A modeling study was conducted to study the effect of incorporating (emim [Tf_2N]) and (emim[CF_3SO_3]) ionic liquids in a polymer matrix using the Maxwell, Lewis–Nielson, and Maxwell–Wagner–Sillar (MWS) gas separation models. The study showed a local agglomeration of SAPO-34 particles and a high deviation from the experimental results. Modification of the MWS model to include the wet phase factor showed good agreement with the experimental results [92]. Sen et al. [93] investigated the impregnation of carbon in polyetherimide using in situ carbonization to tailor SAPO-34 MMMs. Owing to the incompatibility, the impregnated carbon particles redecorated the interfacial pores formed between the filler and polymer. This approach minimized the interfacial pores/defects, which enhanced membrane performance.

2.1.3. SAPO-34 MMMs and Operating Conditions

The operating conditions are one of the key factors affecting membrane performance. Sodeifian et al. [94] investigated the influence of pressure and inclusion of SAPO-34 nanoparticles. The study showed that increasing the pressure (0.4–1.4 MPa) caused an increase in CO_2 permeability, whereas CH_4 and N_2 permeability remained constant. Increasing SAPO-34 within the polyurethane matrix decreases the permeability of CO_2 and CH_4 and

enhanced the ideal selectivity of CO_2/N_2 and CO_2/CH_4, which indicated the benefit of SAPO-34 particle incorporation in the PU matrix, as shown in Figure 4.

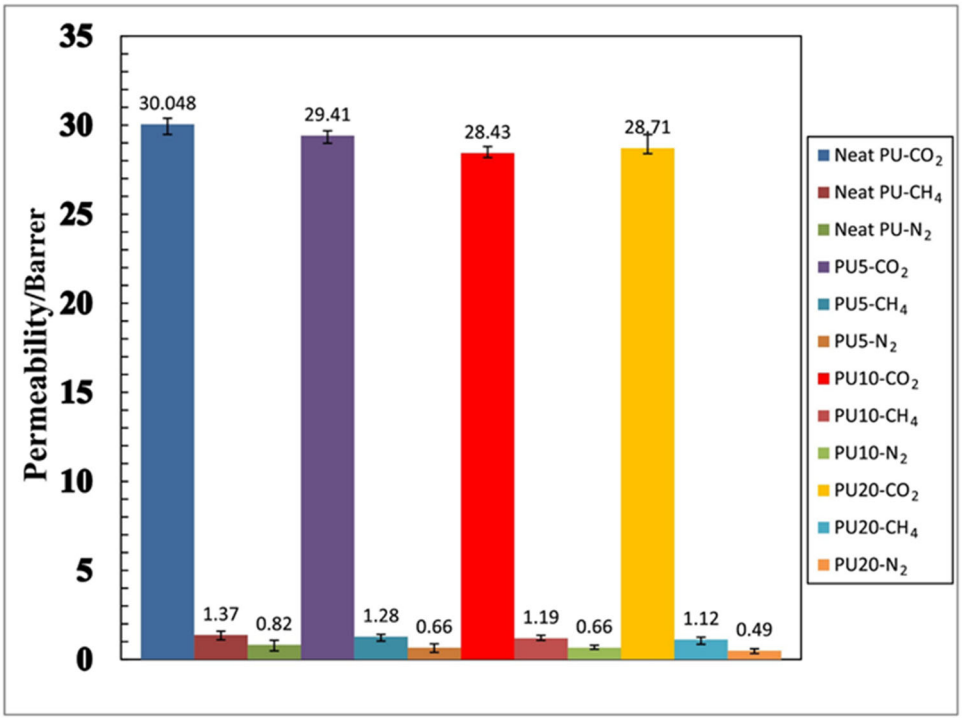

Figure 4. Effect of SAPO-34 content in the gas permeation properties of polyurethane–SAPO-34 membranes on the permeability of CO_2, CH_4, and N_2 gases in 1.2 MPa pressure and selectivity of CO_2/CH_4 and CO_2/N_2 gases in 1.2 MPa pressure. Adapted with permission from Ref. [94]. Copyright 2019 Elsevier.

Rabiee et al. [95] investigated the effects of temperature and pressure on the separation performance of SAPO-34/Pebax MMMs. The study showed that the incorporation of SAPO-34 led to an enhancement in gas permeability, and the membranes exhibited diffusion-dominant behavior, and indicated the molecular sieving effect of SAPO-34. An increase in operating conditions and pressure (4–24 bar) led to an enhancement in gas permeation, increasing the driving force and solution diffusion mechanism. The temperature alternation also showed the same behavior, which increased the Pebax chain mobility around the filler. The above discussions are summarized in Table 1.

Table 1. Summary of separation performance for SAOP-34 MMMs.

Filler	Substrate	CO_2 Permeance	CO_2/CH_4 Selectivity	CO_2/N_2 Selectivity	Ref.
Neat	Matrimid 5218	4.4 Barrer	34	-	[77]
SAPO-34 2 wt%	Matrimid 5218	4.5 Barrer	41.98	-	[77]
SAPO-34 5 wt%	Matrimid 5218	4.6 Barrer	44.24	-	[77]
SAPO-34 10 wt%	Matrimid 5218	5.3 Barrer	50.82	-	[77]
SAPO-34 15 wt%	Matrimid 5218	5.9 Barrer	58.14	-	[77]
SAPO-34 20 wt%	Matrimid 5218	6.9 Barrer	66.99	-	[77]
Neat	Polyethersulfone (PESU)	6.7 Barrer	37.8	-	[78]
SAPO-34 NP 20 wt%	Polyethersulfone (PESU)	8.2 Barrer	42.6	-	[78]
SAPO-34 NP 30 wt%	Polyethersulfone (PESU)	8.9 Barrer	48.3	-	[78]
Neat	Matrimid 5218	9.5 ± 1.07 GPU	29.81	13.63	[79]
SAPO-34 10 wt% uncalcined	Matrimid 5218	7.63 ± 0.81 GPU	31.79	26.31	[79]
SAPO-34 10 wt% calcined	Matrimid 5218	12.5 ± 1.3 GPU	9.32	10.50	[79]
Neat	Polyetherimide	6×10^{-10} mol/(m^2 s Pa)	0.02	-	[80]

Table 1. *Cont.*

Filler	Substrate	CO_2 Permeance	CO_2/CH_4 Selectivity	CO_2/N_2 Selectivity	Ref.
SAPO-34 5 wt%	Polyetherimide	4.4×10^{-10} mol/(m^2 s Pa)	60	-	[80]
SAPO-34 10 wt%	Polyetherimide	6×10^{-10} mol/(m^2 s Pa)	8	-	[80]
Neat	Pebax 1657	100 Barrer	16.7	53.8	[81]
SAPO-34 23 wt%	Pebax 1657	134 Barrer	21.7	55.2	[81]
SAPO-34 33 wt%	Pebax 1657	252 Barrer	17	55	[81]
SAPO-34 50 wt%	Pebax 1657	339 Barrer	16.8	53.2	[81]
Neat	Polysulfone (Asymmetric)	22.0 ± 3.42 GPU	17.3	16.5	[82]
SAPO-34 5 wt%	Polysulfone (Asymmetric)	205.9 ± 7.26 GPU	22.5	21.4	[82]
SAPO-34 10 wt%	Polysulfone (Asymmetric)	314.0 ± 4.65 GPU	28.2	26.1	[82]
SAPO-34 20 wt%	Polysulfone (Asymmetric)	281.18 ± 6.92 GPU	10.9	10.7	[82]
SAPO-34 30 wt%	Polysulfone (Asymmetric)	232. ± 3.21 GPU	3	2.9	[82]
Neat	Polysulfone (Asymmetric)	105 GPU	15	13	[83]
SAPO-34 10 wt%	Polysulfone (Asymmetric)	459 GPU	27	21	[83]
SAPO-34E 10 wt%	Polysulfone (Asymmetric)	706 GPU	31	28	[83]
SAPO-34I 10 wt%	Polysulfone (Asymmetric)	775 GPU	28	22	[83]
Neat	Polyhexafluoropropylene (PHFP)	290 Barrer	14.1	-	[76]
SAPO-34 NP 24.6 v%	Polyhexafluoropropylene (PHFP)	468 Barrer	15.8	-	[76]
SAPO-34 NP 36 v%	Polyhexafluoropropylene (PHFP)	437 Barrer	17.5	-	[76]
Neat	PES	4.45 Barrer	33.2	-	[84]
HMA 10%	PES	0.8 Barrer	32.3	-	[84]
SAPO-34 20 wt%	PES	5.7 Barrer	37	-	[84]
SAPO-34 20 wt% + HMA 10%	PES	1.3 Barrer	44.7	-	[84]
HMA 4%	PES	5.1 Barrer	39.3	-	[85]
SAPO-34 20 wt%	PES	13.8 Barrer	32.7	-	[85]
SAPO-34 20 wt% + HMA 4%	PES	7.8 Barrer	41.6	-	[85]
SAPO-34	PES	18 GPU	1.2	-	[86]
SAPO-34 20 wt%	PES	30 GPU	1.3	-	[86]
SAPO-34 20 wt% m-EDA	PES	10.0 GPU	12.14	-	[86]
SAPO-34 20 wt%	PES	50 GPU	2.5	-	[87]
SAPO-34 20 wt%/IL	PES	0.03 GPU	4.9	-	[87]
SAPO-34 20 wt% m-EDA/IL	PES	0.09 GPU	26.5	-	[87]
SAPO-34 20 wt% m-HA/IL	PES	0.045 GPU	37.2	-	[87]
Neat	Polysulfone (PSf)	21.3 ± 2.8 GPU	17.2	-	[88]
SAPO-34 10 wt%	Polysulfone (PSf)	317.0 ± 3.5 GPU	27.9	-	[88]
SAPO-34 20 wt%	Polysulfone (PSf)	283.0 ± 2.2 GPU	10.8	-	[88]
SAPO-34 10 wt% + 0.5 wt%HFDS	Polysulfone (PSf)	310.4 ± 1.7 GPU	30.4	-	[88]
SAPO-34 10 wt% + 1 wt%HFDS	Polysulfone (PSf)	278.8 ± 2.1 GPU	38.9	-	[88]
SAPO-34 10 wt% + 1.5 wt%HFDS	Polysulfone (PSf)	259.7 ± 4.2 GPU	37.3	-	[88]
SAPO-34 20 wt% + 0.5 wt%HFDS	Polysulfone (PSf)	332.1 ± 5.5 GPU	11.9	-	[88]
SAPO-34 20 wt% + 1 wt%HFDS	Polysulfone (PSf)	293.7 ± 4.9 GPU	27.5	-	[88]
SAPO-34 20 wt% + 1.5 wt%HFDS	Polysulfone (PSf)	306.8 ± 5.2 GPU	24.8	-	[88]
SAPO-34 5 wt%	Polysulfone (PSf)	6.1 GPU	4.9	5.1	[90]
SAPO-34 5 wt%/IL(0.2 M)	Polysulfone (PSf)	24.89 GPU	35.06	40.15	[90]
Neat	Polysulfone (PSf)	5.60 ± 0.75 GPU	3.24	6.15	[91]
SAPO-34 5 wt%	Polysulfone (PSf)	6.53 ± 1.22 GPU	3.47	5.67	[91]
SAPO-34 5 wt%/IL(0.4 M)	Polysulfone (PSf)	4.82 ± 1.28 GPU	4.86	8.04	[91]

Table 1. *Cont.*

Filler	Substrate	CO_2 Permeance	CO_2/CH_4 Selectivity	CO_2/N_2 Selectivity	Ref.
SAPO-34 5 wt%/IL(0.6 M)	Polysulfone (PSf)	7.24 ± 1.78 GPU	20.35	18.82	[91]
SAPO-34 20 wt%	Polyethersulfone (PES)	85.7 GPU	20.67	-	[92]
SAPO-34 20 wt% + IL 5 wt%	Polysulfone (PSf)	230.8 GPU	-	46.20	[92]
SAPO-34 20 wt% + IL 10 wt%	Polysulfone (PSf)	255.69 GPU	-	58.83	[92]
SAPO-34 20 wt% + IL 15 wt%	Polysulfone (PSf)	279.2 GPU	-	60.62	[92]
SAPO-34 20 wt% + IL 20 wt%	Polysulfone (PSf)	300.0 GPU	-	62.58	[92]
Neat	Polyetherimide	3.8×10^{-10} mol/(m^2 s Pa)	-	2.23	[94]
SAPO-34 10 wt%	Polyetherimide	2.8×10^{-8} mol/(m^2 s Pa)	-	2.54	[94]
SAPO-34 25 wt% + Carbonization	Polyetherimide	8.42×10^{-8} mol/(m^2 s Pa)	-	6.47	[94]
SAPO-34 40 wt%	Polyetherimide	9.1×10^{-7} mol/(m^2 s Pa)	-	5.05	[94]
Neat	Polyurethane	30.05 Barrer	21.93	36.64	[89]
SAPO-34 NP 5 wt%	Polyurethane	29.41 Barrer	22.97	44.56	[89]
SAPO-34 NP 10 wt%	Polyurethane	28.43 Barrer	23.89	54.67	[89]
SAPO-34 NP 20 wt%	Polyurethane	28.71 Barrer	25.63	58.59	[89]
Neat	Pebax 1074	120 Barrer	17.5	60.3	[95]
SAPO-34 5 wt%	Pebax 1074	123 Barrer	18.5	61	[95]
SAPO-34 10 wt%	Pebax 1074	130 Barrer	22	62.5	[95]
SAPO-34 20 wt%	Pebax 1074	152 Barrer	29	68	[95]
SAPO-34 30 wt%	Pebax 1074	156 Barrer	35	69	[95]

2.2. Pure SAPO-34 Membranes

The separation properties of mixed-matrix membranes for gas mixtures are unique because of their selective extraction of CO_2, high efficiency, and flexibility. However, harsh operating conditions (high pressure and temperature) are applied to the membranes in real applications, leading to degradation of membrane performance. To overcome this challenge, the use of pure SAPO-34 as a zeolite membrane offers a promising route for achieving superior separation performance. In addition to its unique mechanical, thermal, and chemical stabilities, SAPO-34 is distinguished by competitive CO_2 adsorption and extraordinary molecular sieving. However, the fabrication of pure SAPO-34 membranes requires a substrate to support the membrane. Stainless steel and alumina (disks, tubes, and hollow fibers) are the most frequently reported supports for pure SPAO membranes.

2.2.1. SAPO-34/Alumina Membranes

Since the first paper on using alumina as a support for pure SAPO-34 membranes, extensive work has been conducted to improve membrane performance. The first SAPO-34/alumina membrane was reported in 1997 by Lixiong et al. [96]. A defect-free membrane was fabricated via in situ synthesis. The membrane exhibited a CO_2 permeance of 29.9×10^{-8} mol/(m^2 s Pa) with a CO_2/N_2 selectivity of 11.17. Poshusta et al. [97] reported SAPO-34 crystals supported on the inner walls of α-alumina tubes. The influences of temperature and pressure on single and mixed gases were investigated. The membrane showed CO_2/CH_4 ideal selectivities of 30 and 19 for mixed and single gases, respectively. Following a previous study, Poshusta et al. [98] fabricated another SAPO-34 membrane with a slight modification of the synthesis temperature. The membrane showed a high CO_2 permeance for CO_2 and a constant CO_2/CH_4 selectivity. Single gas permeation was governed by a molecular sieve, whereas mixed gas was governed by competitive adsorption. A facile, cost-effective, and less toxic waste synthesis method for SAPO-30/alumina membranes was reported by Zhou et al. [99]. The synthesis used only one template (TEAOH) and $Al(OH)_3$ instead of Al(O-i-Pr)$_3$. Figure 5 shows the microstructure analysis of SAPO-34 cubic crystals with a 1–3 μm crystal size and 3 μm membrane thickness. The formation of impermeable

regions as a result of the synthesis gel was overcome by rinsing with deionized water for 24 h, followed by calcination. The membrane exhibited high separation properties for CO_2. Carreon et al. reported an SAPO-34 membrane with a thinner SAPO layer (6–7.5 µm) fabricated using the secondary seeded growth method, which showed high performance in a single gas permeation [100].The performance enhancement was related to the small size of the zeolite crystals, structural properties of the support, and layer/support interactions. Li and Fan [101] investigated the modification of crystallization time. The reported membrane exhibited 1.2×10^{-6} mol/m^2 s Pa CO_2 permeance with (CO_2/N_2 ratio of 32) a (50/50) mixture. A high selectivity stability was achieved under wet conditions with 8% water vapor and a 37% decline in CO_2 permeance. Ion exchange was described as an effective route to enhance permeation performance by Chew et al. [102]. The microwave heating approach was reported to fabricate SAPO-34 membranes by ion-exchanging SAPO-34 with alkaline earth cations (Ba, Sr, Mg, and Ca). Ba-SAPO-34 showed the best result, with a 240% improvement in CO_2/CH_4 selectivity for equimolar mixture. The same group conducted a modeling study using a central composite design CCD and response surface methodology RSM to study the impact of the operating conditions on CO_2 permeance and CO_2/CH_4 selectivity [103].

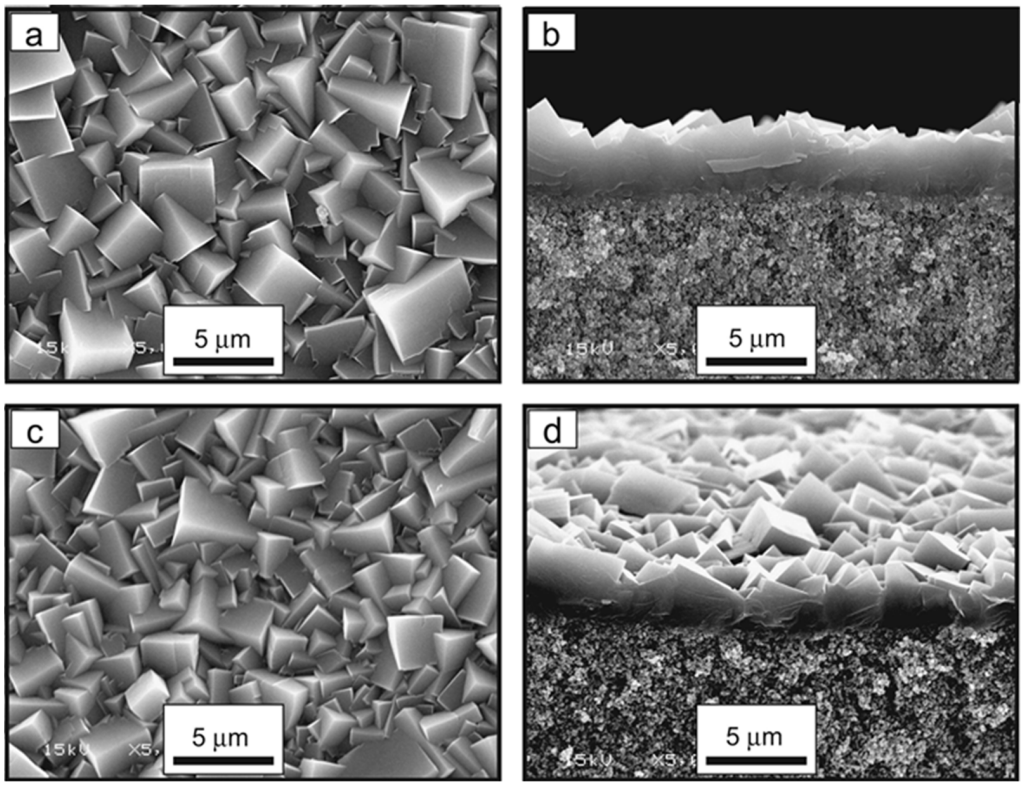

Figure 5. Surface and cross-sectional SEM images of SAPO-34 membranes prepared with $Al(OH)_3$ and $TEAOH/P_2O_5$ ratios of 1.75 (**a**,**b**) and 2.0 (**c**,**d**). Adapted with permission from Ref. [99]. Copyright 2013 Elsevier.

Furthermore, they investigated the separation performance at low CO_2 concentrations. The membrane showed good stability and durability with CO_2 permeance of 17.5×10^{-7} mol/m^2·s·Pa and CO_2/N_2 selectivity of 78 for 5% CO_2 on the feed side [104]. Li et al. [105] demonstrated the dip-coating effect of a thin layer of carbon/SAPO-34 using permeation analysis. This selectivity enhancement was ascribed to the permeation blockage of the non-absorbable gas. Shi et al. [106] reported, for the first time, a rapid free organic template synthesis method for SAPO-34 membrane on α-Al_2O_3 disk. The new approach enhanced the performance of membrane 1.2 times as compared with organic template membranes. The enhancement was attributed to the avoidance of defects in the

membrane formed by the organic template after high-temperature calcination. SAPO-34/α-Al_2O_3 disk membranes were prepared by seeded growth using the microwave irradiation method for the first time by Liu et al. [107]. This synthesis route led to a homogenous, thin, and dense SAPO-34 layer on the α-alumina disk, which improved the separation properties. A strategy to prepare non-zeolitic pores on SAPO-34 membranes was highlighted by Das et al. [108] by the insertion of Pd nanoparticles. This strategy led to an enhancement in membrane quality for separation applications. As shown in Figure 6, the reduction in H_2 permeance for Pd-SAPO-34 membranes as compared with unmodified membranes indicated the successful repair of non-zeolitic pores by Pd nanoparticles. However, the CO_2 permeance remained almost stable at different feed pressures, confirming that the CO_2 permeance on Pd-SAPO-34 membranes is a molecular sieving process. Thus, the selectivity for H_2/CO_2 was enhanced by up to 20.8 for Pd membranes as compared with unmodified membranes [108]. Wu et al. [109] studied the permeation analysis of (SSZ-13 and SAPO-34) membranes in a propane atmosphere. The orientation of SAPO-34 seed crystals played a more significant role in membrane performance than random orientation.

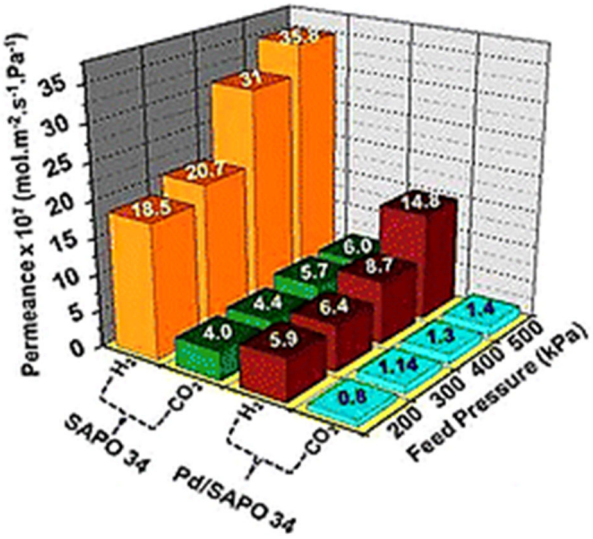

Figure 6. H_2/CO_2 separation performance on Pd/SAPO-34 membranes. Adapted with permission from Ref. [108]. Copyright 2019 Royal Society of Chemistry.

Bing et al. [110] reported a spin-coated highly oriented SAPO-34 seed layer, and a well-intergrown oriented SAPO-34 membrane was fabricated by secondary microwave hydrothermal growth. This approach led to high-quality membranes with no large defects, which improved the membrane performance. Kgaphola et al. [111] reporteda nanocomposite SAPO-34 membrane fabricated by a pore-plugging hydrothermal PPH approach for post-combustion CO_2 capture. The PPH approach provided high mechanical and thermal stability as compared with the hydrothermal and seeded growth methods. In addition, PPH minimized the high-temperature thermal expansion mismatch. Song et al. [112] fabricated a defect-free SAPO-34/alumina tube membrane by seeded growth under microwave irradiation. Different factors that affect the morphology and membrane structure were investigated, including the seed size, heating mode, aging, and synthesis time. The membrane performance under simulated power-plant flue gas was investigated by Liu et al. [113]. The membrane exhibited a high separation performance under dry conditions. However, 19.3% and 14.9% performance decline were observed under humid conditions. A facile defect healing strategy using vacuum-assisted deposition (VAD) for SAPO-34/alumina membranes was proposed by Mu et al. [114]. This strategy was effective in healing the nonselective defects of the membrane during preparation without affecting the CO_2 permeance and significantly improving the CO_2/CH_4 selectivity. A bis(triethoxysilyl)ethane (BTESE)-derived organosilica was used for healing. In addition, the effects of pressure,

temperature, and healing cycles were investigated. More cycles of healing via VAD caused a decrease in the membrane performance, indicating the low CO_2 permeance and selectivity of BTESE. Recently, Wang et al. [115] fabricated highly oriented SAPO-34 nanofilms with ordered channels (prepared by the gel-nuclei-less method) on α-Al_2O_3 tubes via a secondary growth route. The superior performance was related to the large and continuous area of the nanofilms, which provided a fast permeating and CO_2 selective route.

2.2.2. SAPO-34/Stainless Steel Membranes

Li et al. reported the in situ crystallization of SAPO-34 membranes using tubular stainless steel with 0.8 µm pores. A CO_2/CH_4 selectivity of 270 and a CO_2 permeance of 2.4×10^{-7} mol/(m^2 s Pa) were achieved [116]. They also studied the influence of impurities (N_2, H_2O, C_2H_4, C_3H_8, and n-C_4H_{10}) on the membrane performance [117]. This study revealed that N_2 had an insignificant impact on membrane performance. The introduction of light HCs caused a decline in permeation performance, which was related to the higher heat of adsorption in C_4. However, reversible performance recovery was observed after removing impurities. The ratio of (Si/Al gel) was investigated by Li et al. [118] where a membrane with a Si/Al gel ratio of 0.15 showed the highest CO_2 permeance and selectivity for CO_2/CH_4. Venna et al. [119] fabricated oriented thin SAPO-34/stainless-steel membranes via a seeded growth approach. This method was the main reason for the high membrane performance CO_2/CH_4 selectivity of 9 and CO_2 permeance of 2.5×10^{-6} mol/(m^2 s Pa) Functionalization of SAPO seeds with different organic amino cations (EDA, HA, and octylamine) has been reported. The EDA-functionalized membrane showed high performance as compared with the unfunctionalized membrane and other modified membranes. The preferential adsorption of CO_2 was a key factor for performance improvement.

2.2.3. SAPO-34/Silica Membranes

Silica can also be used as a substrate in SAPO-34 membranes. Makertihartha et al. [120] reported a defect-free SAPO-34 membrane fabricated via two methods: optimized secondary growth (combined rubbing/aging) and rubbing. The first approach showed higher CO_2/N_2 selectivity, which was attributed to the defect-free and continuous membrane layer. Owing to the concentration polarization phenomenon at higher pressures, the membrane exhibited two N_2 flux regions. Table 2 summarizes the application of pure SAPO-34 membranes in natural gas purification and air separation.

Table 2. Summary of separation performances for pure SAOP-34 membranes.

Filler	Substrate	CO_2 Permeance	CO_2/CH_4 Selectivity	CO_2/N_2 Selectivity	Ref.
SAPO-34	Stainless steel	2×10^{-7} mol/(m^2 s Pa)	270	-	[116]
SAPO-34 (M1)	Stainless steel	1.1×10^{-7} mol/(m^2 s Pa)	27	-	[117]
SAPO-34 (M2)	Stainless steel	1.4×10^{-7} mol/(m^2 s Pa)	54	-	[117]
SAPO-34 (M3)	Stainless steel	1.4×10^{-7} mol/(m^2 s Pa)	87	-	[117]
SAPO-34 (M3)	Stainless steel	4.9×10^{-8} mol/(m^2 s Pa)	55	-	[117]
SAPO-34	Stainless steel tube	1.2×10^{-7} mol/(m^2 s Pa)	170	-	[118]
SAPO-34	Stainless steel	2.52×10^{-6} mol/(m^2 s Pa)	9.30	-	[119]
SAPO-34 (nonfunctionalized)	Stainless steel	4.6×10^{-7} mol/(m^2 s Pa)	159	29	[119]
SAPO-34 (0.15 mmol of HA)	Stainless steel	3.7×10^{-7} mol/(m^2 s Pa)	238	36	[119]
SAPO-34 (0.15 mmol of OA)	Stainless steel	1.9×10^{-7} mol/(m^2 s Pa)	229	30	[119]

Table 2. *Cont.*

Filler	Substrate	CO_2 Permeance	CO_2/CH_4 Selectivity	CO_2/N_2 Selectivity	Ref.
SAPO-34 (0.15 mmol of ED)	Stainless steel	5×10^{-7} mol/(m^2 s Pa)	245	39	[119]
SAPO-34	α-Al_2O_3 disk	6.40×10^{-8} mol/(m^2 s Pa)	-	4.16	[96]
SAPO-34	α-Al_2O_3 disk	29.9×10^{-8} mol/(m^2 s Pa)	-	11.17	[119]
SAPO-34	α-Al_2O_3 tubes	2.4×10^{-8} mol/(m^2 s Pa)	19	5.7	[97]
SAPO-34	α-Al_2O_3 tubes	15.5×10^{-8} mol/(m^2 s Pa)	20	7.1	[98]
SAPO-34	α-Al_2O_3	1.2×10^{-6} mol/(m^2 s Pa)	70	-	
SAPO-34	α-Al_2O_3	1.8×10^{-6} mol/(m^2 s Pa)	171	-	[100]
SAPO-34	α-Al_2O_3	1.2×10^{-6} mol/(m^2 s Pa)	-	32	[101]
SAPO-34	α-Al_2O_3	0.45×10^{-6} mol/(m^2 s Pa)	-	9.5	[101]
SAPO-34	α-Al_2O_3	0.7×10^{-7} mol/(m^2 s Pa)	-	10	[101]
Ba-SAPO-34	α-Al_2O_3 tubes	37.6×10^{-8} mol/(m^2 s Pa)	103	-	[102]
Ba-SAPO-34	α-Al_2O_3 tubes	17×10^{-8} mol/(m^2 s Pa)	36	-	[102]
SAPO-34	α-Al_2O_3 disk	17.5×10^{-7} mol/(m^2 s Pa)	-	78	[104]
SAPO-34	α-Al_2O_3 disk	8.1×10^{-7} mol/(m^2 s Pa)	-	25.1	[104]
Thin carbon/SAPO-34	α-Al_2O_3 tubes	8.7×10^{-8} mol/(m^2 s Pa)	87	-	[105]
SAPO-34	seven-channel monolith Al_2O_3	3.7×10^{-7} mol/(m^2 s Pa)	21	-	[121]
SAPO-34	seven-channel monolith Al_2O_3	6.3×10^{-7} mol/(m^2 s Pa)	44	-	[121]
SAPO-34	seven-channel monolith Al_2O_3	6.3×10^{-7} mol/(m^2 s Pa)	56	-	[121]
SAPO-34	α-Al_2O_3 disk	1.63×10^{-6} mol/(m^2 s Pa)	258	-	[106]
SAPO-34	α-Al_2O_3 disk	1.72×10^{-6} mol/(m^2 s Pa)	213	-	[106]
SAPO-34	α-Al_2O_3 disk	1.26×10^{-6}	95	-	[107]
SAPO-34	α-Al_2O_3 tubes	1.5×10^{-6} mol/(m^2 s Pa)	100	-	[109]
SAPO-34	α-Al_2O_3 tubes	5×10^{-7} mol/(m^2 s Pa)	100	-	[109]
SAPO-34	α-Al_2O_3	1.57×10^{-6} mol/(m^2 s Pa)	109	-	[110]
SAPO-34	α-Al_2O_3 tubes	2.44×10^{-7} mol/(m^2 s Pa)	-	7.9	[111]
SAPO-34	α-Al_2O_3	6.2×10^{-7} mol/(m^2 s Pa)	89	-	[112]
SAPO-34	α-Al_2O_3 tubes	1.82×10^{-6} mol/(m^2 s Pa)	-	32.9	[113]
SAPO-34	α-Al_2O_3 tubes	4.67×10^{-7} mol/(m^2 s Pa)	-	10.3	[113]
SAPO-34	α-Al_2O_3 tubes (untreated)	2.5×10^{-7} mol/(m^2 s Pa)	61	-	[114]
SAPO-34	α-Al_2O_3 tubes (treated)	2.4×10^{-7} mol/(m^2 s Pa)	158	-	[114]
SAPO-34	α-Al_2O_3 tubes	$27 \pm 1.41 \times 10^{-7}$ mol/(m^2 s Pa)	146 ± 5.6	-	[122]
SAPO-34	α-Al_2O_3 tubes	1.2×10^{-5} mol/(m^2 s Pa)	135	41	[115]
SAPO-34	α-Al_2O_3/(4CHF)	1.18×10^{-6} mol/(m^2 s Pa)	160	-	[123]
SAPO-34	α-Al_2O_3/(4CHF)	2.3×10^{-7} mol/(m^2 s Pa)	53		[124]
SAPO-34/PDMS	α-Al_2O_3/(4CHF)	1.18×10^{-7} mol/(m^2 s Pa)	68	-	[124]
SAPO-34/PDMS	α-Al_2O_3/(4CHF)	4.2×10^{-7} mol/(m^2 s Pa)	86	-	[124]

Table 2. *Cont.*

Filler	Substrate	CO_2 Permeance	CO_2/CH_4 Selectivity	CO_2/N_2 Selectivity	Ref.
SAPO-34	α-Al_2O_3/(4CHF)	1.7×10^{-8} mol/(m^2 s Pa)	0.9	-	[125]
SAPO-34/PDMS	α-Al_2O_3/(4CHF)	1.18×10^{-6} mol/(m^2 s Pa)	160	-	[125]
SAPO-34	Silica tubes	2.01×10^{-6} mol/(m^2 s Pa)	-	53	[120]
SAPO-34	Silica tubes	2.01×10^{-6} mol/(m^2 s Pa)	-	2.08	[120]

2.2.4. Scale-Up and Industrial Approach of Pure SAPO-34 Membranes

In practical applications, it is necessary to develop membranes with high performance and low fabrication costs. Hollow fiber supports have been demonstrated to be a better alternative to disk and tubular supports. A few attempts have shown promising results in the scalability aspect of SAPO-34 membranes, including the study that conducted by S. Li and coworkers [101]. The study demonstrated the scalability of SAPO-34 membrane on a porous tubular stainless-steel support from 5 cm to 25 cm, which was optimized. Crystallization time, gel composition, and precursor were optimized to acquire the same membrane performance of 5 cm SAPO-34 membrane. Additionally, the fabrication cost was reduced by using low-cost aluminum sources. Despite the challenges in scalability of pure SAPO-34 membranes, hollow fiber-based route offers an alternative approach for scalability [126]. Recently, B. Wang et al. [50] reported a simple and controllable scale-up fabrication method for SAPO-34 on commercial α-alumina tubular support. The dilution of mother liquid had a vital impact in the synthesis method. The membrane exhibited ultra-high CO_2 permeance and CO_2/CH_4 selectivity as compared with the typical membrane.

Chen et al. [123] fabricated an SAPO-34 membrane on α-Al_2O_3 four-channel hollow fibers (4CHF) via a secondary growth method. An excellent performance was achieved, which was related to the transfer resistance of the support. Furthermore, the synthesis parameters (temperature and time) were investigated. The study showed that the synthesis temperature improved the separation selectivity at the expense of the CO_2 permeance, which was attributed to the increasing thickness. Furthermore, the synthesis time showed that membrane performance increased with time. However, at a certain point, the reverse effect was observed, which might have been related to the crystal dissolution of the zeolite layer. Rehman et al. reported a facile strategy to overcome the degradation of SAPO-34 membrane performance by water interaction [124]. It was based on the dip coating of the membrane in α-, ω-dihydroxypolydimethylsiloxane (PDMS) to provide surface protection. In addition to protection, the modification enhanced the membrane performance under wet and dry conditions as compared with unmodified membranes. In addition, the study showed that PDMS protected the membrane, and the performance of the membrane did not change too much (5–8%) after half-year storage, although a 71% decline in CO_2 permeance and 85% in CO_2/CH_4 selectivity were observed for unmodified membrane. Another report by Rehman et al. investigated a hydrophobic modification of the SAPO-34/4 CHF membrane. The study reported the use of n-dodecyltrimethoxysilane as a surface modifier for membranes with superior selectivity as compared with unmodified membranes under wet conditions [125]. Ping et al. reported a scale-up study [121] where SAPO-34 was prepared by seeded-gel synthesis on seven-channel monolithic alumina supports. They systematically studied the effects of different monolithic supports (single and seven channels) and different seeding methods (dip coating, rub coating, and seeded gel). The seeded gel on the seven-channel monolith support showed the best performance, which was ascribed to the permeate flow rates through the monoliths. In addition, the seed-gel approach reduced the cost and time required to prepare zeolite membranes.

3. Summary and Outcome

In the last decade, extensive research progress in SAPO-34 membranes has led to high-performance membranes. The development of molecular sieve membranes made of

SAPO-34 zeolite for CO_2 separation from the air and natural gas has made great progress. Pure inorganic and MMMs are summarized in this review. Based on the literature, SAPO-34 membranes are mostly studied for possible applications in natural gas purification and its separation from air. Previously, it has also been studied for hydrogen separation and catalytic membrane reactors for elevated temperature reactions. However, a number of directions have to be investigated and studied to further improve the SAPO-34 membranes for industrial applications. Thus, there is still room for boosting the performance of SAPO-34 membranes. This review highlights the following research viewpoints for further studies:

1. Rigid pore membranes and ion-exchange membranes must be developed to increase the solubility and rejection of particular gases.
2. More studies should be focus on the transport mechanism of MMMs and pure SAPO-34 membranes.
3. Regarding techno-economic analysis, the economics of each separation method must be evaluated in terms of factors such as cost per kilogram of product and energy consumption per kilogram, with a view to encourage and explore the research in this direction.
4. In hydrogen separation using Pd-based membrane, SAPO-34 interlayer can play an important role as a diffusion barrier and substrate modifier over the support. SAPO-34 membranes were prepared on α-Al_2O_3 four-channel hollow fiber (4CHF) supported by secondary growth method. Moreover, the 4CHF supported SAPO-34 membranes could also provide high membrane packing density for membrane modules and cut fabrication costs, which is a promising candidate for practical applications. Therefore, more work is required to explore its application in Pd-based membranes by using vacuum-assisted seeding and secondary growth methods on the different substrates.
5. Regarding He separation applications, SAPO-34 membranes are less explored in helium separation from He/CH_4 since this is one the most attractive separations; due to size sieving and diffusivity difference, SAPO-34 membrane surpassed the Robeson limit upper bound, making these membranes appealing for the recovery of helium from natural gas.
6. In natural gas purification, SAPO-34 is one of the best candidates due to its unique pore size and adsorption capabilities. However, it decomposes over the time (years) due to the presence of moisture in the raw natural gas. Therefore, it is recommended to improve its moisture resistance property by modifying its surface using hydrophobic barrier. The chemical modification strategy of SAPO-34 would strengthen the properties of the membranes. More studies of this type are required in SAPO-34 membrane research for boosting membrane steadiness and performances under high humidity conditions.
7. Regarding defect-free membranes, thin SAPO-34 membranes over the supports have been produced through various synthetic strategies to reduce defects; however, it is extremely challenging to obtain defect-free membranes. Many studies have been attempted to heal these defects using post-treatments, but some methods are costly and some result in producing thicker membranes which ultimately lower the permeance. Therefore, more work is required to heal the defects of SAPO-34 membranes by carefully designing the post-synthetic modifications that should balance the resultant membranes' cost and permeance.
8. The demand of the scaling up of mixed matrix membranes is a hot topic. However, the commercialization of the SAPO-34-based MMMs is still in the early stage and requires more work to develop facile synthetic methods with cost effective techniques. Scaling up the Pure SAPO-34 membranes is a pivotal requirement for industrial commercialization. However, systematic optimization of the fabrication parameter is required to acquire the scaling-up procedure. Pure SAPO-34 thin membranes are produced on solid supports. However, they face many challenges when it comes to scaling-up their fabrication on longer tubular supports (more than 20 cm). In large-scale production, these membranes might require better approaches such as modified

synthetic schemes and big autoclaves, etc. These approaches are reviewed in the above sections. The scalability of SAPO-34 membranes and mixed matrix membranes are still in the early stage and need more investigation and development in the scalability aspect before reaching the commercialization stage. Thus, more efforts are needed to produce longer SAPO-34 membranes before being implemented at an industrial scale. Hollow-fiber-based module systems could provide an alternative pathway owing to their large area to volume ratios.

9. The high cost of the SAPO-34 zeolite membrane modules as compared with the polymeric membranes is one barrier to implementing these membranes in the industry for real practical applications. The cost in synthesizing SAPO-34 or zeolite membranes comes mainly from templates, Al/Si sources, and supports. A limited number of research studies have reported an alternative synthesis approach using low-priced alumina and/or template-free synthesis. The entire membrane cost consists of the zeolite filler and membrane support. As a result, research activities should consider choosing and fabricating less expensive membrane supports. Therefore, more studies are required to seek a cost-effective synthesis approach for SAPO-34 membranes to achieve cost-effective, scalability, and stability SAPO-34 membranes. In addition, improvement of SAPO-34 membrane toward industrial implementation at high operating conditions should be considered.

Funding: This research was funded by the Deanship of Research Oversight and Coordination (DROC) at King Fahd University of Petroleum and Minerals (KFUPM) through project no. DF181004.

Institutional Review Board Statement: Not applicable.

Informed Consent Statement: Not applicable.

Data Availability Statement: Not applicable.

Acknowledgments: The author would like to acknowledge the support provided by the Deanship of Research Oversight and Coordination (DROC) at King Fahd University of Petroleum and Minerals (KFUPM) for funding this work through project no. DF181004.

Conflicts of Interest: The author declares no conflict of interest.

References

1. Burns, T.D.; Pai, K.N.; Subraveti, S.G.; Collins, S.P.; Krykunov, M.; Rajendran, A.; Woo, T.K. Prediction of MOF Performance in Vacuum Swing Adsorption Systems for Postcombustion CO_2 Capture Based on Integrated Molecular Simulations, Process Optimizations, and Machine Learning Models. *Environ. Sci. Technol.* **2020**, *54*, 4536–4544. [CrossRef] [PubMed]
2. Usman, M.; Iqbal, N.; Noor, T.; Zaman, N.; Asghar, A.; Abdelnaby, M.M.; Galadima, A.; Helal, A. Advanced strategies in Metal-Organic Frameworks for CO_2 Capture and Separation. *Chem. Rec.* **2021**. [CrossRef]
3. Garba, M.D.; Usman, M.; Khan, S.; Shehzad, F.; Galadima, A.; Ehsan, M.F.; Ghanem, A.S.; Humayun, M. CO_2 towards fuels: A review of catalytic conversion of carbon dioxide to hydrocarbons. *J. Environ. Chem. Eng.* **2021**, *9*, 104756. [CrossRef]
4. Dindi, A.; Quang, D.V.; Vega, L.F.; Nashef, E.; Abu-Zahra, M.R.M. Applications of fly ash for CO_2 capture, utilization, and storage. *J. CO_2 Util.* **2019**, *29*, 82–102. [CrossRef]
5. Khan, S.; Khulief, Y.A.; Al-Shuhail, A.A. Effects of reservoir size and boundary conditions on pore-pressure buildup and fault reactivation during CO_2 injection in deep geological reservoirs. *Environ. Earth Sci.* **2020**, *79*, 294. [CrossRef]
6. Khan, S.; Khulief, Y.A.; Al-Shuhail, A.A. Numerical Modeling of the Geomechanical Behavior of Biyadh Reservoir Undergoing CO_2 Injection. *Int. J. Geomech.* **2017**, *17*, 04017039. [CrossRef]
7. Song, C.; Liu, Q.; Deng, S.; Li, H.; Kitamura, Y. Cryogenic-based CO_2 capture technologies: State-of-the-art developments and current challenges. *Renew. Sust. Energ. Rev.* **2019**, *101*, 265–278. [CrossRef]
8. Yousef, A.M.; El-Maghlany, W.M.; Eldrainy, Y.A.; Attia, A. New approach for biogas purification using cryogenic separation and distillation process for CO_2 capture. *Energy* **2018**, *156*, 328–351. [CrossRef]
9. Tengku Hassan, T.N.A.; Shariff, A.M.; Mohd Pauzi, M.M.i.; Khidzir, M.S.; Surmi, A. Insights on Cryogenic Distillation Technology for Simultaneous CO_2 and H2S Removal for Sour Gas Fields. *Molecules* **2022**, *27*, 1424. [CrossRef]
10. Breck, D.W.; Breck, D.W. *Zeolite Molecular Sieves: Structure, Chemistry, and Use*; John Wiley & Sons: New York, NY, USA, 1973.
11. Yaseen, M.; Humayun, M.; Khan, A.; Usman, M.; Ullah, H.; Tahir, A.A.; Ullah, H. Preparation, Functionalization, Modification, and Applications of Nanostructured Gold: A Critical Review. *Energies* **2021**, *14*, 1278. [CrossRef]

12. Usman, M.; Humayun, M.; Shah, S.S.; Ullah, H.; Tahir, A.A.; Khan, A.; Ullah, H. Bismuth-Graphene Nanohybrids: Synthesis, Reaction Mechanisms, and Photocatalytic Applications—A Review. *Energies* **2021**, *14*, 2281. [CrossRef]
13. Usman, M.; Humayun, M.; Garba, M.D.; Ullah, L.; Zeb, Z.; Helal, A.; Suliman, M.H.; Alfaifi, B.Y.; Iqbal, N.; Abdinejad, M.; et al. Electrochemical Reduction of CO_2: A Review of Cobalt Based Catalysts for Carbon Dioxide Conversion to Fuels. *Nanomaterials* **2021**, *11*, 2029. [CrossRef] [PubMed]
14. Israf Ud, D.; Qazi, N.; Mustapha, D.G.; Abdulrahman, I.A.; Mshari, A.A.; Muhammad, U. A Review of Preparation Methods for Heterogeneous Catalysts. *Mini-Rev. Org. Chem.* **2022**, *19*, 92–110. [CrossRef]
15. Humayun, M.; Zada, A.; Li, Z.; Xie, M.; Zhang, X.; Qu, Y.; Raziq, F.; Jing, L. Enhanced visible-light activities of porous BiFeO3 by coupling with nanocrystalline TiO_2 and mechanism. *Appl. Catal. B* **2016**, *180*, 219–226. [CrossRef]
16. Humayun, M.; Ullah, H.; Tahir, A.A.; bin Mohd Yusoff, A.R.; Mat Teridi, M.A.; Nazeeruddin, M.K.; Luo, W. An Overview of the Recent Progress in Polymeric Carbon Nitride Based Photocatalysis. *Chem. Rec.* **2021**. [CrossRef]
17. Humayun, M.; Ullah, H.; Usman, M.; Habibi-Yangjeh, A.; Tahir, A.A.; Wang, C.; Luo, W. Perovskite-type lanthanum ferrite based photocatalysts: Preparation, properties, and applications. *J. Energy Chem.* **2022**, *66*, 314–338. [CrossRef]
18. Helal, A.; Usman, M.; Arafat, M.E.; Abdelnaby, M.M. Allyl functionalized UiO-66 metal-organic framework as a catalyst for the synthesis of cyclic carbonates by CO_2 cycloaddition. *J. Ind. Eng. Chem.* **2020**, *89*, 104–110. [CrossRef]
19. Yaqoob, L.; Noor, T.; Iqbal, N.; Nasir, H.; Sohail, M.; Zaman, N.; Usman, M. Nanocomposites of cobalt benzene tricarboxylic acid MOF with rGO: An efficient and robust electrocatalyst for oxygen evolution reaction (OER). *Renew. Energy* **2020**, *156*, 1040–1054. [CrossRef]
20. Ullah, L.; Zhao, G.; Xu, Z.; He, H.; Usman, M.; Zhang, S. 12-Tungstophosphoric acid niched in Zr-based metal-organic framework: A stable and efficient catalyst for Friedel-Crafts acylation. *Sci. China Chem.* **2018**, *61*, 402–411. [CrossRef]
21. Ullah, L.; Zhao, G.; Ma, J.-X.; Usman, M.; Khan, R.; Hedin, N. Pd-promoted heteropolyacid on mesoporous zirconia as a stable and bifunctional catalyst for oxidation of thiophenes. *Fuel* **2022**, *310*, 122462. [CrossRef]
22. Usman, M.; Zhu, J.; Chuiyang, K.; Arslan, M.T.; Khan, A.; Galadima, A.; Muraza, O.; Khan, I.; Helal, A.; Al-Maythalony, B.A.; et al. Propene Adsorption-Chemisorption Behaviors on H-SAPO-34 Zeolite Catalysts at Different Temperatures. *Catalysts* **2019**, *9*, 919. [CrossRef]
23. Arslan, M.T.; Qureshi, B.A.; Gilani, S.Z.A.; Cai, D.; Ma, Y.; Usman, M.; Chen, X.; Wang, Y.; Wei, F. Single-Step Conversion of H2-Deficient Syngas into High Yield of Tetramethylbenzene. *ACS Catal.* **2019**, *9*, 2203–2212. [CrossRef]
24. Zhu, J.; Li, Y.; Muhammad, U.; Wang, D.; Wang, Y. Effect of alkene co-feed on the MTO reactions over SAPO-34. *Chem. Eng. J.* **2017**, *316*, 187–195. [CrossRef]
25. Ma, Y.; Cai, D.; Li, Y.; Wang, N.; Muhammad, U.; Carlsson, A.; Tang, D.; Qian, W.; Wang, Y.; Su, D.; et al. The influence of straight pore blockage on the selectivity of methanol to aromatics in nanosized Zn/ZSM-5: An atomic Cs-corrected STEM analysis study. *RSC Adv.* **2016**, *6*, 74797–74801. [CrossRef]
26. Usman, M.; Li, D.; Razzaq, R.; Yaseen, M.; Li, C.; Zhang, S. Novel MoP/HY catalyst for the selective conversion of naphthalene to tetralin. *J. Ind. Eng. Chem.* **2015**, *23*, 21–26. [CrossRef]
27. Wang, H.; Cao, Y.; Li, D.; Muhammad, U.; Li, C.; Li, Z.; Zhang, S. Catalytic hydrorefining of tar to liquid fuel over multi-metals (W-Mo-Ni) catalysts. *J. Renew. Sustain. Energy* **2013**, *5*, 053114. [CrossRef]
28. Zhang, H.H.; Cao, Y.M.; Usman, M.; Li, L.J.; Li, C.S. Study on the Hydrotreating Catalysts Containing Phosphorus of Coal Tar to Clean Fuels. *Adv. Mat. Res.* **2012**, *531*, 263–267. [CrossRef]
29. Kan, T.; Sun, X.; Wang, H.; Li, C.; Muhammad, U. Production of Gasoline and Diesel from Coal Tar via Its Catalytic Hydrogenation in Serial Fixed Beds. *Energy Fuels* **2012**, *26*, 3604–3611. [CrossRef]
30. Li, D.; Zhang, H.; Usman, M.; Li, Z.; Han, L.; Li, C.; Zhang, S. Study on the hydrotreatment of C9 aromatics over supported multi-metal catalysts on γ-Al_2O_3. *J. Renew. Sustain. Energy* **2014**, *6*, 033132. [CrossRef]
31. Lok, B.M.; Messina, C.A.; Patton, R.L.; Gajek, R.T.; Cannan, T.R.; Flanigen, E.M. Silicoaluminophosphate molecular sieves: Another new class of microporous crystalline inorganic solids. *J. Am. Chem. Soc.* **1984**, *106*, 6092–6093. [CrossRef]
32. Song, S.; Gao, F.; Zhang, Y.; Li, X.; Zhou, M.; Wang, B.; Zhou, R. Preparation of SSZ-13 membranes with enhanced fluxes using asymmetric alumina supports for N_2/CH_4 and CO_2/CH_4 separations. *Sep. Purif. Technol.* **2019**, *209*, 946–954. [CrossRef]
33. Liu, H.; Gao, X.; Wang, S.; Hong, Z.; Wang, X.; Gu, X. SSZ-13 zeolite membranes on four-channel α-Al2O3 hollow fibers for CO_2 separation. *Sep. Purif. Technol.* **2021**, *267*, 118611. [CrossRef]
34. Kalipcilar, H.; Bowen, T.C.; Noble, R.D.; Falconer, J.L. Synthesis and Separation Performance of SSZ-13 Zeolite Membranes on Tubular Supports. *Chem. Mater.* **2002**, *14*, 3458–3464. [CrossRef]
35. Hasegawa, Y.; Abe, C.; Natsui, M.; Ikeda, A. Gas Permeation Properties of High-Silica CHA-Type Zeolite Membrane. *Membranes* **2021**, *11*, 249. [CrossRef]
36. Liang, L.; Zhu, M.; Chen, L.; Zhong, C.; Yang, Y.; Wu, T.; Wang, H.; Kumakiri, I.; Chen, X.; Kita, H. Single Gas Permeance Performance of High Silica SSZ-13 Zeolite Membranes. *Membranes* **2018**, *8*, 43. [CrossRef]
37. Dai, W.; Wang, C.; Dyballa, M.; Wu, G.; Guan, N.; Li, L.; Xie, Z.; Hunger, M. Understanding the Early Stages of the Methanol-to-Olefin Conversion on H-SAPO-34. *ACS Catal.* **2015**, *5*, 317–326. [CrossRef]
38. Nishiyama, N.; Kawaguchi, M.; Hirota, Y.; Van Vu, D.; Egashira, Y.; Ueyama, K. Size control of SAPO-34 crystals and their catalyst lifetime in the methanol-to-olefin reaction. *Appl. Catal. A-Gen.* **2009**, *362*, 193–199. [CrossRef]

39. Sun, Q.; Xie, Z.; Yu, J. The state-of-the-art synthetic strategies for SAPO-34 zeolite catalysts in methanol-to-olefin conversion. *Natl. Sci. Rev.* **2017**, *5*, 542–558. [CrossRef]
40. Yang, Z.; Zhang, L.; Zhou, Y.; Wang, H.; Wen, L.; Kianfar, E. Investigation of effective parameters on SAPO-34 nanocatalyst in the methanol-to-olefin conversion process: A review. *Rev. Inorg. Chem.* **2020**, *40*, 91–105. [CrossRef]
41. Yang, G.; Han, J.; Huang, Y.; Chen, X.; Valtchev, V. Busting the efficiency of SAPO-34 catalysts for the methanol-to-olefin conversion by post-synthesis methods. *Chin. J. Chem. Eng.* **2020**, *28*, 2022–2027. [CrossRef]
42. Ahmad, M.S.; Cheng, C.K.; Bhuyar, P.; Atabani, A.E.; Pugazhendhi, A.; Chi, N.T.L.; Witoon, T.; Lim, J.W.; Juan, J.C. Effect of reaction conditions on the lifetime of SAPO-34 catalysts in methanol to olefins process—A review. *Fuel* **2021**, *283*, 118851. [CrossRef]
43. Askari, S.; Bashardoust Siahmard, A.; Halladj, R.; Miar Alipour, S. Different techniques and their effective parameters in nano SAPO-34 synthesis: A review. *Powder Technol.* **2016**, *301*, 268–287. [CrossRef]
44. Nasser, G.A.; Muraza, O.; Nishitoba, T.; Malaibari, Z.; Al-Shammari, T.K.; Yokoi, T. OSDA-free chabazite (CHA) zeolite synthesized in the presence of fluoride for selective methanol-to-olefins. *Micrpor. Mesopor. Mater.* **2019**, *274*, 277–285. [CrossRef]
45. Nasser, G.A.; Muraza, O.; Nishitoba, T.; Malaibari, Z.; Yamani, Z.H.; Al-Shammari, T.K.; Yokoi, T. Microwave-Assisted Hydrothermal Synthesis of CHA Zeolite for Methanol-to-Olefins Reaction. *Ind. Eng. Chem. Res.* **2019**, *58*, 60–68. [CrossRef]
46. Salih, H.A.; Muraza, O.; Abussaud, B.; Al-Shammari, T.K.; Yokoi, T. Catalytic Enhancement of SAPO-34 for Methanol Conversion to Light Olefins Using in Situ Metal Incorporation. *Ind. Eng. Chem. Res.* **2018**, *57*, 6639–6646. [CrossRef]
47. Nasser, G.A.; Al-Qadri, A.A.; Jamil, A.K.; Bakare, I.A.; Sanhoob, M.A.; Muraza, O.; Yamani, Z.H.; Yokoi, T.; Saleem, Q.; Alsewdan, D. Conversion of Methanol to Olefins over Modified OSDA-Free CHA Zeolite Catalyst. *Ind. Eng. Chem. Res.* **2021**, *60*, 12189–12199. [CrossRef]
48. Liang, J.; Li, H.; Zhao, S.; Guo, W.; Wang, R.; Ying, M. Characteristics and performance of SAPO-34 catalyst for methanol-to-olefin conversion. *Appl. Catal.* **1990**, *64*, 31–40. [CrossRef]
49. Yu, L.; Nobandegani, M.S.; Hedlund, J. Industrially relevant CHA membranes for CO_2/CH_4 separation. *J. Membr. Sci.* **2022**, *641*, 119888. [CrossRef]
50. Wang, B.; Huang, W.; Zhu, Y.; Zhou, R.; Xing, W. Ultra-permeable high-selective SAPO-34 membranes for efficient CO_2 capture. *J. Membr. Sci.* **2022**, *650*, 120420. [CrossRef]
51. Wang, B.; Wang, N.; Li, X.; Zhou, R.; Xing, W. Exfoliation of lamellar SAPO-34 zeolite to nanosheets and synthesis of thin SAPO-34 membranes by a nanosheet-seeded secondary growth approach. *J. Membr. Sci.* **2022**, *645*, 120177. [CrossRef]
52. Ahmed, A.; Ishiguro, S.; Seshimo, M.; Subramanian, B.; Matsukata, M. Synthesis of SAPO-34 Membrane and Its Application to the Separation of Water/Acetic Acid Mixtures by Vapor Permeation. *J. Chem. Eng. Jpn.* **2022**, *55*, 97–104. [CrossRef]
53. Liu, Z.; Xu, S.; Hao, J.; Song, L.; Chong, M.; Cheng, D.-G.; Chen, F. Bifunctional catalysts composed of low silicon-content SAPO-34 nanosheets and In_2O_3/ZrO_2 with improved performance for CO_2 hydrogenation. *Greenh. Gases Sci. Technol.* **2022**, *12*, 305–320. [CrossRef]
54. Usman, M.; Ghanem, A.S.; Ali Shah, S.N.; Garba, M.D.; Khan, M.Y.; Khan, S.; Humayun, M.; Khan, A.L. A review on SAPO-34 zeolite materials for CO_2 capture and conversion. *Chem. Rec.* **2022**, e202200039. [CrossRef]
55. Xu, J.; Haw, K.-G.; Li, Z.; Pati, S.; Wang, Z.; Kawi, S. A mini-review on recent developments in SAPO-34 zeolite membranes and membrane reactors. *React. Chem. Eng.* **2021**, *6*, 52–66. [CrossRef]
56. Rimaz, S.; Kosari, M.; Zarinejad, M.; Ramakrishna, S. A comprehensive review on sustainability-motivated applications of SAPO-34 molecular sieve. *J. Mater. Sci.* **2022**, *57*, 848–886. [CrossRef]
57. Kumar, S.; Srivastava, R.; Koh, J. Utilization of zeolites as CO_2 capturing agents: Advances and future perspectives. *J. CO_2 Util.* **2020**, *41*, 101251. [CrossRef]
58. Perez, E.V.; Kalaw, G.J.D.; Ferraris, J.P.; Balkus, K.J.; Musselman, I.H. Amine-functionalized (Al) MIL-53/VTEC™ mixed-matrix membranes for $H2/CO_2$ mixture separations at high pressure and high temperature. *J. Membr. Sci.* **2017**, *530*, 201–212. [CrossRef]
59. Bastani, D.; Esmaeili, N.; Asadollahi, M. Polymeric mixed matrix membranes containing zeolites as a filler for gas separation applications: A review. *J. Ind. Eng. Chem.* **2013**, *19*, 375–393. [CrossRef]
60. Davoodabadi, A.; Mahmoudi, A.; Ghasemi, H. The potential of hydrogen hydrate as a future hydrogen storage medium. *iScience* **2021**, *24*, 101907. [CrossRef]
61. Ackley, M.W. Medical oxygen concentrators: A review of progress in air separation technology. *Adsorption* **2019**, *25*, 1437–1474. [CrossRef]
62. Marwat, M.A.; Humayun, M.; Afridi, M.W.; Zhang, H.; Abdul Karim, M.R.; Ashtar, M.; Usman, M.; Waqar, S.; Ullah, H.; Wang, C.; et al. Advanced Catalysts for Photoelectrochemical Water Splitting. *ACS Appl. Energy Mater.* **2021**, *4*, 12007–12031. [CrossRef]
63. Elrasheedy, A.; Nady, N.; Bassyouni, M.; El-Shazly, A. Metal Organic Framework Based Polymer Mixed Matrix Membranes: Review on Applications in Water Purification. *Membranes* **2019**, *9*, 88. [CrossRef]
64. Shafiq, S.; Al-Maythalony, B.A.; Usman, M.; Ba-Shammakh, M.S.; Al-Shammari, A.A. ZIF-95 as a filler for enhanced gas separation performance of polysulfone membrane. *RSC Adv.* **2021**, *11*, 34319–34328. [CrossRef]
65. Usman, M.; Ali, M.; Al-Maythalony, B.A.; Ghanem, A.S.; Saadi, O.W.; Ali, M.; Jafar Mazumder, M.A.; Abdel-Azeim, S.; Habib, M.A.; Yamani, Z.H.; et al. Highly Efficient Permeation and Separation of Gases with Metal–Organic Frameworks Confined in Polymeric Nanochannels. *ACS Appl. Mater. Interfaces* **2020**, *12*, 49992–50001. [CrossRef]

66. Husna, A.; Hossain, I.; Jeong, I.; Kim, T.-H. Mixed Matrix Membranes for Efficient CO_2 Separation Using an Engineered UiO-66 MOF in a Pebax Polymer. *Polymers* **2022**, *14*, 655. [CrossRef]
67. Tara, N.; Shamair, Z.; Habib, N.; Craven, M.; Bilad, M.R.; Usman, M.; Tu, X.; Khan, A.L. Simultaneous increase in CO_2 permeability and selectivity by BIT-72 and modified BIT-72 based mixed matrix membranes. *Chem. Eng. Res. Des.* **2022**, *178*, 136–147. [CrossRef]
68. Xiong, S.; Li, L.; Dong, L.; Tang, J.; Yu, G.; Pan, C. Covalent-organic frameworks (COFs)-based membranes for CO_2 separation. *J. CO_2 Util.* **2020**, *41*, 101224. [CrossRef]
69. Khan, N.A.; Humayun, M.; Usman, M.; Ghazi, Z.A.; Naeem, A.; Khan, A.; Khan, A.L.; Tahir, A.A.; Ullah, H. Structural Characteristics and Environmental Applications of Covalent Organic Frameworks. *Energies* **2021**, *14*, 2267. [CrossRef]
70. Kang, Z.; Peng, Y.; Qian, Y.; Yuan, D.; Addicoat, M.A.; Heine, T.; Hu, Z.; Tee, L.; Guo, Z.; Zhao, D. Mixed Matrix Membranes (MMMs) Comprising Exfoliated 2D Covalent Organic Frameworks (COFs) for Efficient CO_2 Separation. *Chem. Mater.* **2016**, *28*, 1277–1285. [CrossRef]
71. Duan, K.; Wang, J.; Zhang, Y.; Liu, J. Covalent organic frameworks (COFs) functionalized mixed matrix membrane for effective CO_2/N_2 separation. *J. Membr. Sci.* **2019**, *572*, 588–595. [CrossRef]
72. Wang, X.; Shi, X.; Wang, Y. In Situ Growth of Cationic Covalent Organic Frameworks (COFs) for Mixed Matrix Membranes with Enhanced Performances. *Langmuir* **2020**, *36*, 10970–10978. [CrossRef]
73. Mittal, G.; Dhand, V.; Rhee, K.Y.; Park, S.-J.; Lee, W.R. A review on carbon nanotubes and graphene as fillers in reinforced polymer nanocomposites. *J. Ind. Eng. Chem.* **2015**, *21*, 11–25. [CrossRef]
74. Kiran, M.D.; Govindaraju, H.K.; Jayaraju, T.; Kumar, N. Review-Effect of Fillers on Mechanical Properties of Polymer Matrix Composites. *Mater. Today Proc.* **2018**, *5*, 22421–22424. [CrossRef]
75. Cai, W.; Xie, J.; Luo, J.; Chen, X.; Wang, M.; Wang, Y.; Li, J. n-Octyltrichlorosilane Modified SAPO-34/PDMS Mixed Matrix Membranes for Propane/Nitrogen Mixture Separation. *Separations* **2022**, *9*, 64. [CrossRef]
76. Santaniello, A.; Di Renzo, A.; Di Maio, F.; Belov, N.A.; Yampolskii, Y.P.; Golemme, G. Competing non ideal behaviour of SAPO-34 and Poly(hexafluoropropylene) in mixed matrix membranes. *Micrpor. Mesopor. Mater.* **2020**, *303*, 110241. [CrossRef]
77. Peydayesh, M.; Asarehpour, S.; Mohammadi, T.; Bakhtiari, O. Preparation and characterization of SAPO-34—Matrimid®5218 mixed matrix membranes for CO_2/CH_4 separation. *Chem. Eng. Res. Des.* **2013**, *91*, 1335–1342. [CrossRef]
78. Wu, T.; Liu, Y.S.; Kumakiri, I.; Tanaka, K.; Chen, X.S.; Kita, H. Preparation and Permeation Properties of PESU-Based Mixed Matrix Membranes with Nano-Sized CHA Zeolites. *J. Chem. Eng. Jpn.* **2019**, *52*, 514–520. [CrossRef]
79. Carter, D.; Tezel, F.H.; Kruczek, B.; Kalipcilar, H. Investigation and comparison of mixed matrix membranes composed of polyimide matrimid with ZIF-8, silicalite, and SAPO-34. *J. Membr. Sci.* **2017**, *544*, 35–46. [CrossRef]
80. Belhaj Messaoud, S.; Takagaki, A.; Sugawara, T.; Kikuchi, R.; Oyama, S.T. Mixed matrix membranes using SAPO-34/polyetherimide for carbon dioxide/methane separation. *Sep. Purif. Technol.* **2015**, *148*, 38–48. [CrossRef]
81. Zhao, D.; Ren, J.Z.; Li, H.; Hua, K.S.; Deng, M.C. Poly(amide-6-b-ethylene oxide)/SAPO-34 mixed matrix membrane for CO_2 separation. *J. Energy Chem.* **2014**, *23*, 227–234. [CrossRef]
82. Junaidi, M.U.M.; Leo, C.P.; Ahmad, A.L.; Kamal, S.N.M.; Chew, T.L. Carbon dioxide separation using asymmetric polysulfone mixed matrix membranes incorporated with SAPO-34 zeolite. *Fuel Process. Technol.* **2014**, *118*, 125–132. [CrossRef]
83. Junaidi, M.U.M.; Khoo, C.P.; Leo, C.P.; Ahmad, A.L. The effects of solvents on the modification of SAPO-34 zeolite using 3-aminopropyl trimethoxy silane for the preparation of asymmetric polysulfone mixed matrix membrane in the application of CO_2 separation. *Micrpor. Mesopor. Mater.* **2014**, *192*, 52–59. [CrossRef]
84. Cakal, U.; Yilmaz, L.; Kalipcilar, H. Effect of feed gas composition on the separation of CO_2/CH_4 mixtures by PES-SAPO 34-HMA mixed matrix membranes. *J. Membr. Sci.* **2012**, *417*, 45–51. [CrossRef]
85. Oral, E.E.; Yilmaz, L.; Kalipcilar, H. Effect of Gas Permeation Temperature and Annealing Procedure on the Performance of Binary and Ternary Mixed Matrix Membranes of Polyethersulfone, SAPO-34, and 2-Hydroxy 5-Methyl Aniline. *J. Appl. Polym. Sci.* **2014**, *131*, 40679. [CrossRef]
86. Ahmad, N.N.R.; Mukhtar, H.; Mohshim, D.F.; Nasir, R.; Man, Z. Effect of different organic amino cations on SAPO-34 for PES/SAPO-34 mixed matrix membranes toward CO_2/CH_4separation. *J. Appl. Polym. Sci.* **2016**, *133*, 43387. [CrossRef]
87. Nasir, R.; Ahmad, N.N.R.; Mukhtar, H.; Mohshim, D.F. Effect of ionic liquid inclusion and amino–functionalized SAPO-34 on the performance of mixed matrix membranes for CO_2/CH_4 separation. *J. Environ. Chem. Eng* **2018**, *6*, 2363–2368. [CrossRef]
88. Junaidi, M.U.M.; Leo, C.P.; Ahmad, A.L.; Ahmad, N.A. Fluorocarbon functionalized SAPO-34 zeolite incorporated in asymmetric mixed matrix membranes for carbon dioxide separation in wet gases. *Micrpor. Mesopor. Mater.* **2015**, *206*, 23–33. [CrossRef]
89. Nawar, A.; Ghaedi, H.; Ali, M.; Zhao, M.; Iqbal, N.; Khan, R. Recycling waste-derived marble powder for CO_2 capture. *Process Saf. Environ. Prot.* **2019**, *132*, 214–225. [CrossRef]
90. Ahmad, N.N.R.; Leo, C.P.; Mohammad, A.W.; Ahmad, A.L. Modification of gas selective SAPO zeolites using imidazolium ionic liquid to develop polysulfone mixed matrix membrane for CO_2 gas separation. *Micrpor. Mesopor. Mater.* **2017**, *244*, 21–30. [CrossRef]
91. Mohshim, D.F.; Mukhtar, H.; Man, Z. The effect of incorporating ionic liquid into polyethersulfone-SAPO34 based mixed matrix membrane on CO_2 gas separation performance. *Sep. Purif. Technol.* **2014**, *135*, 252–258. [CrossRef]
92. Mohshim, D.F.; Mukhtar, H.; Dutta, B.K.; Man, Z. Predicting CO_2 Permeation through an Enhanced Ionic Liquid Mixed Matrix Membrane (IL3M). *Int. J. Chem. Eng.* **2019**, *2019*, 1–10. [CrossRef]

93. Sen, M.; Das, N. In situ carbon deposition in polyetherimide/SAPO-34 mixed matrix membrane for efficient CO_2/CH_4 separation. *J. Appl. Polym. Sci.* **2017**, *134*, 45508. [CrossRef]
94. Sodeifian, G.; Raji, M.; Asghari, M.; Rezakazemi, M.; Dashti, A. Polyurethane-SAPO-34 mixed matrix membrane for CO_2/CH_4 and CO_2/N_2 separation. *Chin. J. Chem. Eng.* **2019**, *27*, 322–334. [CrossRef]
95. Rabiee, H.; Meshkat Alsadat, S.; Soltanieh, M.; Mousavi, S.A.; Ghadimi, A. Gas permeation and sorption properties of poly(amide-12-b-ethyleneoxide)(Pebax1074)/SAPO-34 mixed matrix membrane for CO_2/CH_4 and CO_2/N_2 separation. *J. Ind. Eng. Chem.* **2015**, *27*, 223–239. [CrossRef]
96. Lixiong, Z.; Mengdong, J.; Enze, M. Synthesis of SAPO-34/ceramic composite membranes. In *Studies in Surface Science and Catalysis*; Chon, H., Ihm, S.-K., Uh, Y.S., Eds.; Elsevier: Amsterdam, The Netherlands, 1997; Volume 105, pp. 2211–2216.
97. Poshusta, J.C.; Tuan, V.A.; Falconer, J.L.; Noble, R.D. Synthesis and permeation properties of SAPO-34 tubular membranes. *Ind. Eng. Chem. Res* **1998**, *37*, 3924–3929. [CrossRef]
98. Poshusta, J.C.; Tuan, V.A.; Pape, E.A.; Noble, R.D.; Falconer, J.L. Separation of light gas mixtures using SAPO-34 membranes. *AlChE J.* **2000**, *46*, 779–789. [CrossRef]
99. Zhou, R.F.; Ping, E.W.; Funke, H.H.; Falconer, J.L.; Noble, R.D. Improving SAPO-34 membrane synthesis. *J. Membr. Sci.* **2013**, *444*, 384–393. [CrossRef]
100. Carreon, M.A.; Li, S.; Falconer, J.L.; Noble, R.D. Alumina-supported SAPO-34 membranes for CO_2/CH_4 separation. *J. Am. Chem. Soc.* **2008**, *130*, 5412–5413. [CrossRef]
101. Li, S.; Fan, C.Q. High-Flux SAPO-34 Membrane for CO_2/N_2 Separation. *Ind. Eng. Chem. Res.* **2010**, *49*, 4399–4404. [CrossRef]
102. Li, S.G.; Carreon, M.A.; Zhang, Y.F.; Funke, H.H.; Noble, R.D.; Falconer, J.L. Scale-up of SAPO-34 membranes for CO_2/CH_4 separation. *J. Membr. Sci.* **2010**, *352*, 7–13. [CrossRef]
103. Chew, T.L.; Ahmad, A.L.; Bhatia, S. Microwave heating-synthesized zeolite membrane for CO_2/CH_4 separation. *Desalination Water Treat.* **2012**, *47*, 139–149. [CrossRef]
104. Chew, T.L.; Yeong, Y.F.; Ho, C.D.; Ahmad, A.L. Ion-Exchanged Silicoaluminophosphate-34 Membrane for Efficient CO_2/N_2 Separation with Low CO_2 Concentration in the Gas Mixture. *Ind. Eng. Chem. Res.* **2018**, *58*, 729–735. [CrossRef]
105. Li, G.; Yang, J.H.; Wang, J.Q.; Xiao, W.; Zhou, L.; Zhang, Y.; Lu, J.M.; Yin, D.H. Thin carbon/SAPO-34 microporous composite membranes for gas separation. *J. Membr. Sci.* **2011**, *374*, 83–92. [CrossRef]
106. Shi, H. Organic template-free synthesis of SAPO-34 molecular sieve membranes for CO_2–CH_4 separation. *RSC Adv.* **2015**, *5*, 38330–38333. [CrossRef]
107. Liu, X.; Du, S.; Zhang, B. The seeded growth of dense and thin SAPO-34 membranes on porous α-Al_2O_3 substrates under microwave irradiation. *Mater. Lett.* **2013**, *91*, 195–197. [CrossRef]
108. Das, J.K.; Das, N. Mercaptoundecanoic acid capped palladium nanoparticles in a SAPO 34 membrane: A solution for enhancement of H(2)/CO(2) separation efficiency. *ACS Appl. Mater. Interfaces* **2014**, *6*, 20717–20728. [CrossRef]
109. Falconer, J.; Funke, H.; Noble, R.; Wu, T.; Diaz, M.; Zhou, R.F. Influence of propane on CO_2/CH_4 and N_2/CH_4 separations in CHA zeolite membranes. *Abstr. Pap. Am. Chem. S* **2015**, *249*, 201–209. [CrossRef]
110. Bing, L.C.; Wang, G.J.; Wang, F.; Liu, X.F.; Zhang, B.Q. Preparation of a preferentially oriented SAPO-34 membrane by secondary growth under microwave irradiation. *RSC Adv.* **2016**, *6*, 56170–56173. [CrossRef]
111. Kgaphola, K.; Sigalas, I.; Daramola, M.O. Synthesis and characterization of nanocomposite SAPO-34/ceramic membrane for post-combustion CO_2 capture. *Asia-Pac. J. Chem. Eng.* **2017**, *12*, 894–904. [CrossRef]
112. Song, Q.; Zhang, Y.; Zhang, C.; Zhu, Z.; Gu, X. Diethylamine template-directed synthesis of hollow fiber supported SAPO-34 membranes. *CIESC J.* **2019**, *70*, 2316–2324. [CrossRef]
113. Liu, B.; Tang, C.Y.; Li, X.W.; Wang, B.; Zhou, R.F. High-performance SAPO-34 membranes for CO_2 separations from simulated flue gas. *Micrpor. Mesopor. Mater.* **2020**, *292*, 109712. [CrossRef]
114. Mu, Y.B.; Chen, H.H.; Xiang, H.; Lan, L.; Shao, Y.; Fan, X.L.; Hardacre, C. Defects-healing of SAPO-34 membrane by post-synthesis modification using organosilica for selective CO_2 separation. *J. Membr. Sci.* **2019**, *575*, 80–88. [CrossRef]
115. Wang, B.; Wu, T.; Yu, M.; Li, S.; Zhou, R.; Xing, W. Highly Ordered Nanochannels in a Nanosheet-Directed Thin Zeolite Nanofilm for Precise and Fast CO_2 Separation. *Small* **2020**, *16*, e2002836. [CrossRef] [PubMed]
116. Li, S.G.; Martinek, J.G.; Falconer, J.L.; Noble, R.D.; Gardner, T.Q. High-pressure CO_2/CH_4 separation using SAPO-34 membranes. *Ind. Eng. Chem. Res* **2005**, *44*, 3220–3228. [CrossRef]
117. Tian, Y.Y.; Fan, L.L.; Wang, Z.Y.; Qiu, S.L.; Zhu, G.S. Synthesis of a SAPO-34 membrane on macroporous supports for high permeance separation of a CO_2/CH_4 mixture. *J. Mater. Chem.* **2009**, *19*, 7698–7703. [CrossRef]
118. Li, S.G.; Falconer, J.L.; Noble, R.D. Improved SAPO-34 membranes for CO_2/CH_4 separations. *Adv. Mater.* **2006**, *18*, 2601–2603. [CrossRef]
119. Venna, S.R.; Carreon, M.A. Amino-functionalized SAPO-34 membranes for CO_2/CH_4 and CO_2/N_2 separation. *Langmuir* **2011**, *27*, 2888–2894. [CrossRef]
120. Makertihartha, I.G.B.N.; Kencana, K.S.; Dwiputra, T.R.; Khoiruddin, K.; Mukti, R.R.; Wenten, I.G. Silica supported SAPO-34 membranes for CO_2/N_2 separation. *Micrpor. Mesopor. Mater.* **2020**, *298*, 110068. [CrossRef]
121. Ping, E.W.; Zhou, R.F.; Funke, H.H.; Falconer, J.L.; Noble, R.D. Seeded-gel synthesis of SAPO-34 single channel and monolith membranes, for CO_2/CH_4 separations. *J. Membr. Sci.* **2012**, *415*, 770–775. [CrossRef]

122. Mirfendereski, S.M. RETRACTED: Development of a multi-step hybrid method to synthesize highly-permeable and well-oriented SAPO-34 membranes for CO_2 removal applications. *Chem. Eng. Sci.* **2019**, *208*, 115157. [CrossRef]
123. Chen, Y.; Zhang, Y.; Zhang, C.; Jiang, J.; Gu, X. Fabrication of high-flux SAPO-34 membrane on α-Al_2O_3 four-channel hollow fibers for CO_2 capture from CH 4. *J. CO_2 Util.* **2017**, *18*, 30–40. [CrossRef]
124. Rehman, R.U.; Song, Q.N.; Peng, L.; Wu, Z.Q.; Gu, X.H. A facile coating to intact SAPO-34 membranes for wet CO_2/CH_4 mixture separation. *Chem. Eng. Res. Des.* **2020**, *153*, 37–48. [CrossRef]
125. Rehman, R.U.; Song, Q.N.; Peng, L.; Chen, Y.; Gu, X.H. Hydrophobic modification of SAPO-34 membranes for improvement of stability under wet condition. *Chin. J. Chem. Eng.* **2019**, *27*, 2397–2406. [CrossRef]
126. Wang, Z.; Xu, J.; Pati, S.; Chen, T.; Deng, Y.; Dewangan, N.; Meng, L.; Lin, J.Y.S.; Kawi, S. High H2 permeable SAPO-34 hollow fiber membrane for high temperature propane dehydrogenation application. *AlChE J.* **2020**, *66*, e16278. [CrossRef]